

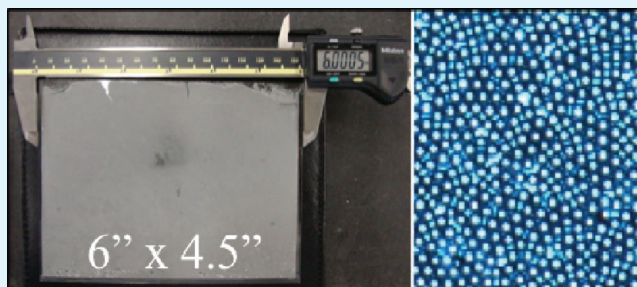
# Rapid Assembly of Colloidal Monolayer for the Synthesis of Surface Anisotropic Particles

Jung Hun (Kevin) Song, David Harbottle, and Jae W. Lee\*

Chemical Engineering Department, The City College of New York, Steinman Hall, 140th Street & Convent Avenue, New York, New York 10031, United States

**ABSTRACT:** A facile and efficient technique for synthesizing rapid and large-scale colloidal monolayer is introduced to obtain surface anisotropic particles. Silica particles grafted with long alkyl chains are rapidly organized into monolayer assemblies by implementing water-film climbing and convective particle assembly on glass slides. Assembled particles are modified into surface-anisotropic particles utilizing physical vapor deposition with a magnetically active material. The magnetic hemisphere enables separation of modified and unmodified surface-anisotropic particles. The proposed methodology can lead to a large-scale production opportunity for surface-anisotropic particles.

**KEYWORDS:** rapid, large-scale, silica, particle, assembly, monolayer, anisotropic, film climbing, separation



## INTRODUCTION

Colloid particles have evolved as an integral component of modern day science and technology.<sup>1–5</sup> These particles encompass wide ranges of applications from synthesis of novel porous materials to photonic band gap materials.<sup>6,7</sup> Most recently, tailoring the functionalities of these particles with multiple facets and properties has gained immense interest for the potential control and addressability in complex systems.<sup>4,5</sup> One such type of multifaceted or anisotropic particles is synthesized through the modification of available surface to result in *Janus* or *Patchy* particles.<sup>4,5</sup> These surface-anisotropic (SA) particles are fabricated with controlled degrees of anisotropy resulting in wide ranges of contrasting properties including, but not limited to hydrophilicity, color, material composition, and magnetic properties.<sup>8,9</sup> The ability to selectively control and apply the desired properties establishes SA particles as highly efficient and effective materials to extend the practicality of colloid particles.

Many novel synthesis techniques to efficiently produce SA particles on a large-scale are being investigated. Some of the techniques include (i) multicompartmental synthesis of particles,<sup>10</sup> (ii) in solution chemical modification targeted surface through masking,<sup>11–13</sup> and (iii) physical or chemical deposition of materials (i.e., metal).<sup>14,15</sup> The synthesis and chemical modification techniques provide a pathway to resolve surface chemical anisotropy, however, these techniques are hindered by limitation and inefficiency to evenly deposit metal on the desired surface as the population of the reactants may not be clearly defined.<sup>12,13,16</sup> The ability to deposit metal on particles is critical as metal-modified SA particles may be applied in catalysis,<sup>14</sup> microelectronics,<sup>5</sup> sensors,<sup>8</sup> and separations<sup>17</sup> among many others. Currently employed and most effective methodology to obtain metal modification has utilized physical vapor deposition of metal.<sup>4,14</sup> Although this technique provides an efficient and reproducible process to synthesize

SA particles,<sup>5</sup> one major drawback is the requirement of monolayer assemblies of particles.

Typical techniques for monolayer production are often characterized by slow large-scale formation, and poor efficiency of coverage and uniformity. Common methods applied in the synthesis of particle monolayers include, but not limited to (i) dip-coating,<sup>1,18,19</sup> (ii) glancing-angle deposition,<sup>20,21</sup> (iii) spin-coating,<sup>22</sup> and (iv) evaporation of a colloid suspension on a substrate.<sup>15</sup> Both dip-coating and glancing-angle are slow assembly techniques with assembly time requiring more than one minute per square inch area.<sup>14</sup> In addition, the processes require precise control over a wide range of parameters including particle concentration and external conditions (i.e., ambient temperature and humidity).<sup>21</sup> Any variations in these conditions may result in a compromise in the assembly quality and rate of the monolayer formation. The downfall of spin-coating arises from a large excess of particle solution required to obtain the monolayer assembly. As the substrate is rotated, the majority of the solution is spun to the outer edges of the substrate, where it ultimately falls from the surface and is discarded. Lastly, the evaporation technique provides minimal control over the deposition rate as the assembly/evaporation is solely guided by external conditions, and often results in multilayer formation.<sup>15</sup>

To overcome the disadvantages and limitations of synthesizing metal deposited SA particles, we introduce a facile and efficient method for a rapid and large-scale monolayer formation of hydrophobic silica colloids on glass slides. The assemblies of monolayer are surface modified through physical vapor deposition, which results in the formation of amphiphilic (hydrophobic silica and hydrophilic iron/iron oxide) and magnetically (iron oxide)

**Received:** March 10, 2011

**Accepted:** May 23, 2011

**Published:** June 14, 2011

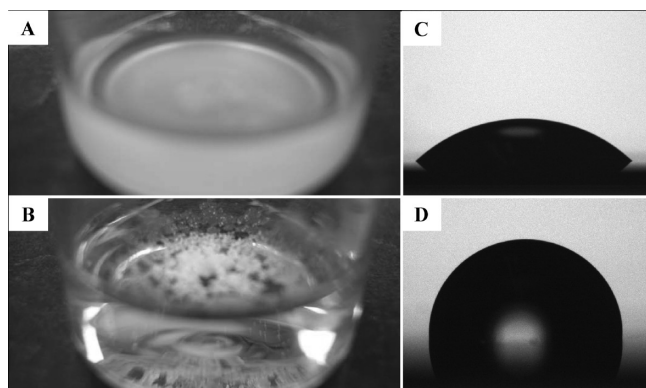


**Figure 1.** Hydrophobic modification of silica particles and silicon wafers. (A) Nongrafted silica particles immersed in DI-water. (B) Dodecanol grafted silica particles suspended at the water–air interface. (C) Contact angle measurement of a water/air/nonmodified silicon interface ( $\sim 44^\circ$  angle). (D) Contact angle measurement of a water/air/grafted silicon interface ( $\sim 95^\circ$  angle).

mobilized SA particles. We show the flexibility of the rapid and large-scale production technique by utilizing hydrophobic sub-micrometer to micrometer-sized silica particles on glass substrates of two different sizes. In addition, a facile pathway to isolate SA modified particles is investigated for the removal of any impurities or non-SA particles.

## EXPERIMENTAL DETAILS

A 25 wt % solution of silica particles, 800 nm (Fuso Chemicals) or  $4\ \mu\text{m}$  (Fiber Optics Center), in 1-dodecanol (Fluka) is formulated in an Erlenmeyer flask in preparation to hydrophobically modify the particle surface (Figure 1A).<sup>23</sup> The flask is attached to a reflux condenser, and the solution is continuously stirred and heated at  $190\ ^\circ\text{C}$  for approximately 7 h. The resulting solution is transferred to a 50 mL centrifuge tube (BD) and centrifuged (Eppendorf) for approximately 5 min. The supernatant of the solution is extracted and discarded. The particle sediments are washed in excess acetone (Acros) via 20 min of ultrasonication (Fisher Scientific). Subsequently, the sonicated solution is centrifuged for 5 min and the supernatant acetone is removed. The particles are further washed with ethanol (Fisher) three times to ensure the complete removal of excess 1-dodecanol. Following the final wash, the particles are dried in a  $60\ ^\circ\text{C}$  vacuum oven for 30 min to obtain hydrophobic silica particles.

Prior to the assembly, microscope glass slides with dimensions of  $3'' \times 1''$  and  $6'' \times 4.5''$  (Corning and Ted Pella) are treated and cleaned with concentrated sulfuric acid (Acros) mixed with NOCHROMIX.<sup>14</sup> The slides are soaked in the acid mixture overnight. Subsequently, the slides are removed and excess acid on the slides is rinsed using DI-water. While the slides are drying, 0.1–0.2 wt % hydrophobic particles are added to DI-water and ultrasonicated for 30 s. Two dried glass slides are temporarily adhered using a thin layer of water and placed in contact with the hydrophobic particle-laden interface. The mixture is gently shaken for 3–5 s to result in monolayer assembly. Repeated shaking of the solution can be performed to ensure full surface coverage of the assembly.

The resulting monolayer assemblies are air-dried and placed in a physical vapor deposition (PVD) unit (Edwards Auto 306) for iron (Fe) deposition (Lesker). Under a high vacuum of  $5 \times 10^{-4}$  Pa,  $80 \pm 10$  nm thick Fe depositions are made with a nominal deposition rate of 3.2 nm/sec. Fe deposited SA particles are removed from the PVD unit and are allowed to oxidize in the ambient condition for 24 h. Oxidized Fe SA particles on glass slides are immersed in DI-water and ultrasonicated for

5 min to remove the particles from the slides. Subsequently, a  $4\ \text{cm}^2$  neodymium magnet is used to separate the modified and unmodified particles. Photographic images are taken using Sony Cyber-shot DSC-W300. Optical and electronic scanning microscope (SEM) images are taken utilizing Nikon AZ300 equipped with 5 megapixel DS-Fi1 camera and Zeiss Supra 55, respectively.

## RESULTS AND DISCUSSION

Some of the most sought after properties or criteria for SA particles include amphiphilicity and mobility. SA particles designed with amphiphilicity show a close resemblance to many surfactant molecules with the advantages of, (i) locating individual “molecules” or particles, and (ii) enhancing the recovery of the particles.<sup>5,12</sup> Furthermore, the incorporation of magnetic materials to the surface modification process introduces mobility to the SA particles, which broadens the impact and applications for potential separation processes.<sup>24</sup>

To obtain the desired characteristics of SA particles, along with addressing the inefficiency of the current synthesis technique, this work reports on an improved metal deposition technique for the synthesis of SA particles. Major advancements addressed are, (i) rapid monolayer formation ( $< 5$  s per microscope slides), (ii) large-scale monolayer formation, (iii) minimized material loss during monolayer formation, and (iv) separation of impurities. Combining all of the advancements, an efficient, rapid, and large-scale synthesis route is achieved.

The fulfillment of relatively large-scale fabrication of SA particles with desired characteristics is achieved in a two-step surface modification. The initial step, hydrophobic modification of silica particles, is performed in preparation to obtain monolayer assemblies and to achieve amphiphilicity. Hydrophobic modification is initiated with the grafting of long alkyl chains onto the silica particles.<sup>25</sup> The grafting comprises of heating an excess alcohol (i.e., 1-dodecanol) with silica particles to replace hydroxide bonds by alkyl bonds at the particle surface (Figure 1A).<sup>26,27</sup> The process has shown to be a facile protocol to convert hydrophilic silica surfaces to hydrophobic surfaces requiring shorter processing time and less stringent surrounding conditions.<sup>25</sup> This grafting step is a crucial precursor to obtain monolayer assembly and amphiphilicity as the subsequent metal deposition reintroduces hydrophilicity to the particle surface.

The wetting behavior of the silica particles pre- and postgrafting of alkyl chains is observed in panels A and B in Figure 1, respectively. Both the unmodified and the grafted silica particles are subjected to DI-water. As apparent from the images, the plain hydrophilic silica particles (Figure 1A) are completely immersed in the DI-water ( $\rho_{\text{silica}} \approx 2.2$  and  $\rho_{\text{water}} \approx 0.998\ \text{g/cm}^3$ ), whereas the grafted silica particles are suspended or floating at the water–air interface confirming the hydrophobic conversion (Figure 1B). To further investigate this hydrophobic modification and onset of wetting behavior, the modification process is duplicated using a silicon wafer (University Wafer), and applied in a contact angle measurement. Silicon wafer with its native oxide layer resembles closely to that of a silica surface and has been utilized as a representative surface.<sup>28</sup> Unmodified silicon wafer (Figure 1C) exhibits average  $43.4^\circ$  contact angle, whereas the grafted silicon wafer (Figure 1D) shows average contact angle of  $94.8^\circ$ , confirming the hydrophobic modification.

Following the conversion, a dense and rapid monolayer assembly is performed utilizing hydrophobic silica particles at



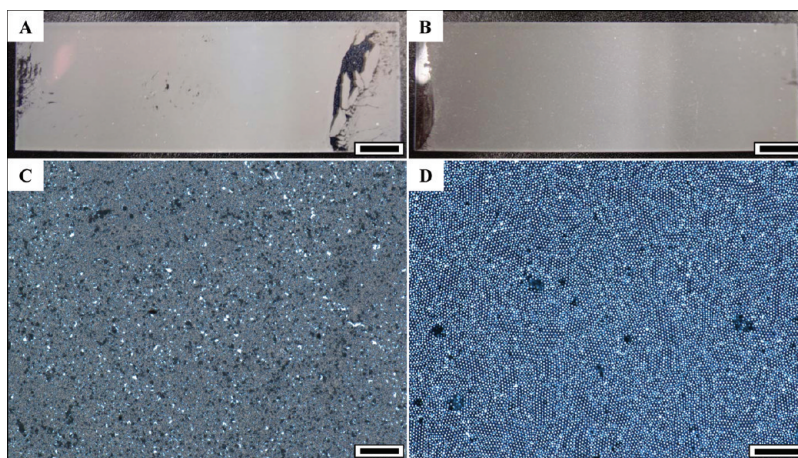


**Figure 2.** Rapid monolayer fabrication using hydrophobic silica particles. (A) Monolayer fabricated using 800 nm hydrophobic silica particles on a glass slide. Scale bar 0.75 cm. (B) Monolayer fabricated using 4  $\mu\text{m}$  hydrophobic silica particles on a glass slide. Scale bar 0.75 cm. (C) Optical microscope image of 800 nm hydrophobic silica particle assembly. Scale bar 50  $\mu\text{m}$ . (D) Optical microscope image of 4  $\mu\text{m}$  hydrophobic silica particle assembly. Scale bar 50  $\mu\text{m}$ .

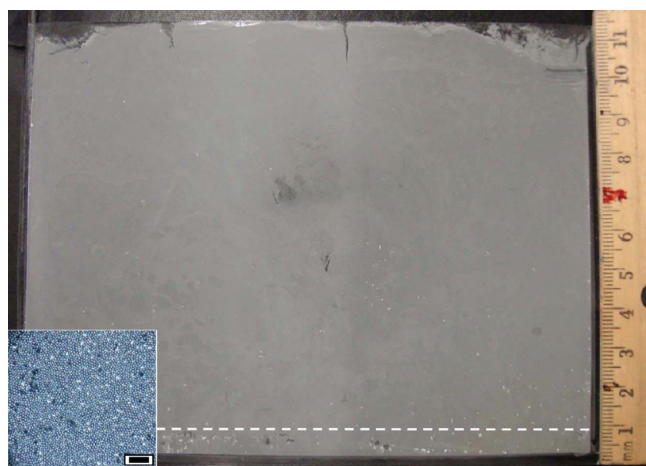


**Figure 3.** Freshly prepared 4  $\mu\text{m}$  hydrophobic silica particles on large 6 in. by 4.5 in. glass slide. White-dotted line depicts the contact line between the glass substrate and the particle-laden water interface. Inset: Optical microscope image of the monolayer sample. Scale bar 40  $\mu\text{m}$ .

the water–air interface. At a selected concentration (0.1 to 0.2 wt %) and with sufficient agitation, the particles are suspended at the water–air interface. Two glass slides are temporarily adhered using a thin-film of water and partially immersed through the interface. The container is gently shaken for approximately 3–5 s. With combined water film-climbing on hydrophilic glass slides and convective assembly of particles,<sup>18,19,29</sup> sub- to close-packed monolayer assemblies on both sides of the adjoined glass slides are formed. Additional shaking is performed, if incomplete coverage is obtained. Following the confirmation of coverage and removal of the monolayer assemblies, the remaining particles ‘reform’ the particle-laden interface inside the container where additional glass slides are introduced to obtain more assemblies. The assembly process is repeated until the particles are depleted. Unlike other monolayer assembly technique,<sup>1,23,30</sup> this closed “one-pot” synthesis technique provides an advantageous pathway to obtain monolayer assembly without any loss of the raw material. Furthermore, this technique provides an efficient

assembly of particles with the capabilities to simultaneously process two substrate surfaces utilizing all of the particles placed in the container.

Photographs of typical assemblies obtained utilizing 800 nm and 4  $\mu\text{m}$  hydrophobic silica particles are shown in Figure 2A and B. Typically, 95–100% surface-coverage is achieved with the applied assembly technique with approximately 85 to 97% of the surface area comprising of monolayer assembly. With the chosen concentration of the particles, approximately 8 to 10 slides of assemblies are obtained within 2 min. In comparison to other assembly techniques aforementioned, this technique illustrates a dramatic reduction in the processing time (approximate reduction of 75–90%).

In depth investigation into the quality of the assembly is performed. Pictures A and B in Figure 2 show areas of multicrystallinity highlighted by minuscule white spots. A further examination through optical microscopy confirms the areas of multicrystallinity as indicated by darker regions in images C and D in Figure 2. As the quality of the resulting SA particles fabricated by PVD is dictated by the available surface of individual particles in a monolayer, determination of the multicrystallinity in the assembly is performed through contrast variation analysis using optical microscope images. Two software, Nikon Elements AR and ImageJ, assisted image analyses to determine the areas of interest. Ten areas of approximately 60  $\text{cm}^2$  are analyzed to determine the quality. On average, monolayer assemblies with particle sizes of 800 nm and 4  $\mu\text{m}$  shows 5.6–15.8% and 2.8–9.5% multicrystallinity, respectively.

The larger percentage with 800 nm particles is attributed to the higher number of particles present per square area resulting in potentially larger number of crystallization sites.<sup>31,32</sup> This fabrication technique results in a similar quality of monolayer in comparison to the reported glancing-angle and dip-coating technique of hydrophobic particle assembly at water–air interface.<sup>23,31,32</sup> In addition, the presence of the visible nonmonolayer particle assemblies can further be reduced or removed by applying a damp cotton cloth to the affected area. Furthermore, an identical protocol is applied to assemble a large-scale monolayer using the 4  $\mu\text{m}$  hydrophobic silica particles on 6 in. by 4.5 in. glass slide as shown in Figure 3. With a larger surface area

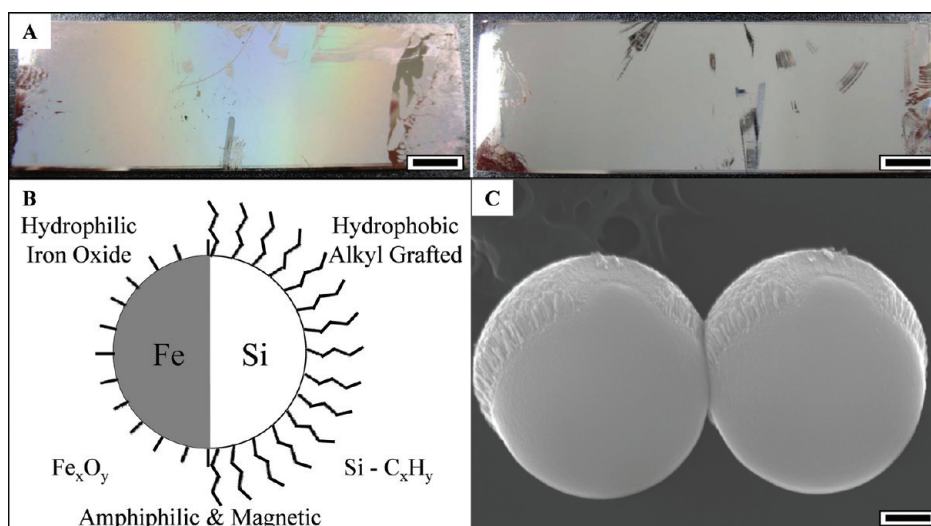


**Figure 4.** Surface-anisotropic particle synthesis. (A) Physical vapor deposition of iron on monolayer assemblies from Figure 2A and B. Scale bars 0.75 cm. (B) Schematic depiction of amphiphilicity and mobility properties introduced to the silica particles. (C) High-resolution scanning electron microscope images of the surface-anisotropic particles with iron deposition. Scale bar 200 nm.

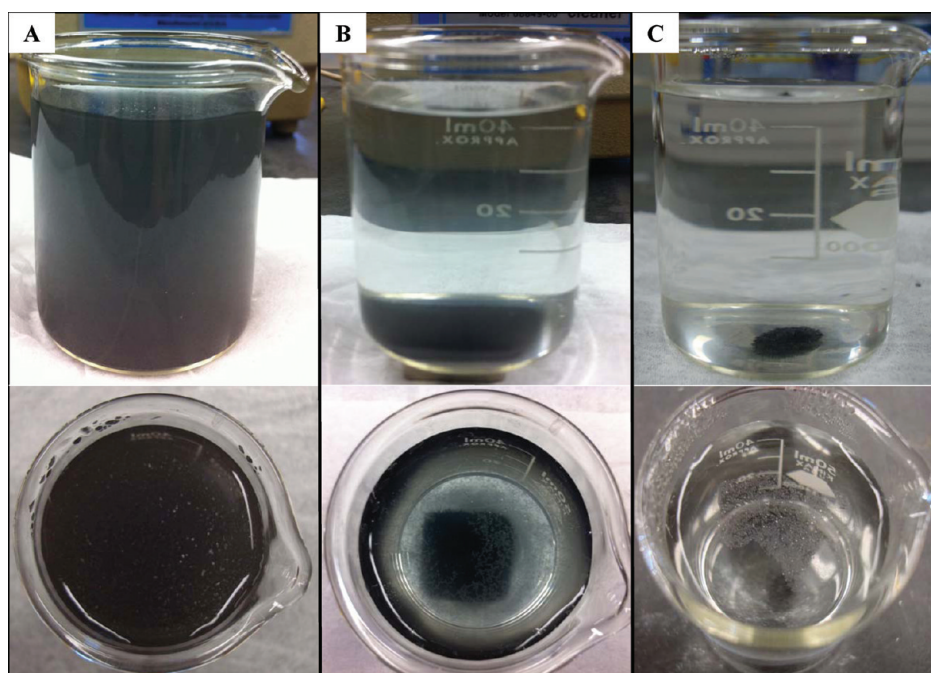


**Figure 5.** Magnetic mobility and separation study of surface-anisotropic particles. (A) Surface-anisotropic particles suspended in DI-water after ultrasonication. (B) Attraction of surface-anisotropic particles to the neodymium magnet. (C) Separation of surface-anisotropic particles to the bottom and unmodified hydrophobic particles suspended at the water–air interface.

(900% increase in comparison to conventional microscope slide), the processing time is increased to approximately 20–30 s per slide. Optical microscope images of both the large-scale assembly (Figure 3 Inset) and the normal glass slide (Figure 2D) show comparable ordering throughout the sample. Increased number of multicrystallinity mainly below the white-dotted line (particle-laden interface contact line) is observed in the large-scale assembly. This increase arises during the removal of the glass slides out of the solution and can be easily removed using a damp cloth.

The introduction of the hydrophilic counterpart and the mobility is achieved through physical vapor deposition (PVD) of magnetic material (Fe) on the particle assemblies.<sup>33,34</sup> As observed in Figure 4A, an even deposition of Fe is performed on the monolayer assemblies utilizing the identical samples depicted in pictures A and B in Figure 2. Directional deposition is introduced by utilizing the PVD technique, which allows deposition of Fe only on one hemisphere of the hydrophobic particle assemblies.<sup>14</sup> The dark reflective nature as a result of the Fe deposition is observed in both slides and minor distortion



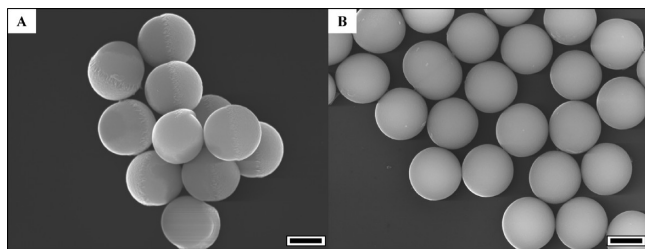


**Figure 6.** (A) Scanning electron microscope image of surface-anisotropic particles extracted from the bottom of the beaker after the magnetic field application. (B) High-resolution image of the unmodified hydrophobic particles from the water–air interface. All scale bars 600 nm.

resulting from handling and scratches is also exhibited. In addition, the light diffraction of visible light (color spectrum) is shown in the 800 nm assembly as an onset of regional close-packing, whereas the 4  $\mu\text{m}$  assembly lacks the diffraction of the visible light due to its larger size.<sup>35,36</sup>

The deposited assemblies are allowed to remain in ambient conditions to induce surface oxidation of Fe. The oxidation of deposition allows an increase in the hydrophilicity to the deposited hemisphere,<sup>24</sup> whereas the alkyl grafting on the opposite hemisphere retains the hydrophobicity to produce the amphiphilicity as illustrated in Figure 4B. The oxidation process takes approximately 24 h, which has shown to be crucial for the structural stability and magnetic activity or mobility of the resulting SA particles.<sup>24</sup>

A high-resolution SEM image of the two oxidized Fe deposited SA particles (800 nm predeposited particles) removed from the original deposition slides is depicted in Figure 4C. As apparent from the image, deposition and thickness of Fe are confirmed in correspondence to the thickness obtained from the PVD unit ( $84 \pm 5$  nm thickness). An apparent variation in the shape of the deposition is observed around the equator of the particles resulting from the shadowing effect by the nearby neighborhood, which confirms the regional close-packed assembly.<sup>6</sup>

With the Fe deposition and subsequent oxidation, a crucial mobile property is incorporated. The magnetic property of the oxidized Fe enables rapid response of the SA particles in the presence of an applied magnetic field.<sup>33</sup> Unmodified hydrophobic particles remain at the water–air interface resulting in the successful separation of SA particles. Figure 5A–C depicts the magnetic separation of the SA particles removed from the glass substrates in DI-water.

The SA particle suspension immediately following the removal from the ultrasonication bath is shown in Figure 5A. A dark SA particle suspension is obtained with spots of unmodified particle aggregation observed at the water–air interface. Subsequently, the solution is subjected to a 4 cm<sup>3</sup> neodymium magnet as shown in Figure 5B. The magnetically active SA particles are drawn toward the strong magnetic field and are isolated into the shape of the magnet. Approximately, 30 s from the application of the magnetic field, all of the SA particles are gathered around the magnet. The magnet is removed and clusters of the SA particles remain at the bottom of the container as shown in Figure 5C. As apparent from the image, unmodified particle clusters are clearly observed at the interface. This separation technique provides another assurance in the quality of the desired SA particles from the process.

To further confirm this separation, both SA and nonmodified particles from respective locations are extracted and examined under SEM. Figure 6A depicts clustering of SA particles without the presence of any unmodified particles, whereas Figure 6B shows only the unmodified particles skimmed from the water–air interface confirming the effectiveness of the SA particle mobility and separation.

## CONCLUSIONS

A reliable fabrication technique for amphiphilic magnetic surface-anisotropic (SA) particles has been introduced. Rapid and large-scale formation of a colloidal monolayer is demonstrated using hydrophobically modified silica particles. The facile monolayer assembly technique has been shown to effectively reduce process timing and increase efficiency by minimizing the loss of raw materials. We have demonstrated that the converted hydrophobic silica particles can be assembled into a monolayer through “one-pot shaking” methodology, with multicrystallinity less than 15%. Furthermore, the particles are successfully deposited with Fe to result in amphiphilic and magnetically active SA particles. With the introduction of applied magnetic field, the converted SA and unmodified plain particles are readily separated, which will ensure only SA particles are recovered. Furthermore, the experimental technique can be tailored to adjust the degree of amphiphilicity and magnetic interaction based on facile substitution of various types of alcohol and magnetic materials.

## AUTHOR INFORMATION

### Corresponding Author

\*Tel: 212-650-6688. FAX: 212-650-6660. E-mail: lee@che.ccnycuny.edu.

## ACKNOWLEDGMENT

The authors thank Dr. Kretzschmar’s lab for initial SEM scans and Dr. Tu’s lab for the usage of auxiliary equipment.

## REFERENCES

- (1) Denkov, N. D.; Velev, O. D.; Kralchevsky, P. A.; Ivanov, I. B.; Yoshimura, H.; Nagayama, K. *Nature* **1993**, *361*, 26–26.
- (2) Aveyard, R.; Binks, B. P.; Clint, J. H. *Adv. Colloid Interface Sci.* **2003**, *100*, 503–546.
- (3) Manoharan, V. N.; Elsesser, M. T.; Pine, D. J. *Science* **2003**, *301*, 483–487.
- (4) Pawar, A. B.; Kretzschmar, I. *Macromol. Rapid Commun.* **2010**, *31*, 150–168.
- (5) Kretzschmar, I.; Song, J. H. *Curr. Opin. Colloid Interface Sci.* **2011**, *16*, 84–95.
- (6) Song, J. H.; Kretzschmar, I. *Langmuir* **2008**, *24*, 10616–10620.
- (7) Subramanian, G.; Manoharan, V. N.; Thorne, J. D.; Pine, D. J. *Adv. Mater.* **1999**, *11*, 1261–1265.
- (8) Perro, A.; Reculosa, S.; Ravaine, S.; Bourgeat-Lami, E. B.; Duguet, E. *J. Mater. Chem.* **2005**, *15*, 3745–3760.
- (9) Nie, Z. H.; Li, W.; Seo, M.; Xu, S. Q.; Kumacheva, E. *J. Am. Chem. Soc.* **2006**, *128*, 9408–9412.
- (10) Roh, K. H.; Martin, D. C.; Lahann, J. *Nat. Mater.* **2005**, *4*, 759–763.
- (11) Pardhy, N. P.; Budhlall, B. M. *Langmuir* **2010**, *26*, 13130–13141.
- (12) Jiang, S.; Chen, Q.; Tripathy, M.; Luijten, E.; Schweizer, K. S.; Granick, S. *Adv. Mater.* **2010**, *22*, 1060–1071.
- (13) Cui, J. Q.; Kretzschmar, I. *Langmuir* **2006**, *22*, 8281–8284.

- (14) Song, J. H.; Kretzschmar, I. *ACS Appl. Mater. Interfaces* **2009**, *1*, 1747–1754.
- (15) Ye, S. R.; Carroll, R. L. *ACS Appl. Mater. Interfaces* **2010**, *2*, 616–620.
- (16) Taylor, R. N. K.; Bao, H. X.; Tian, C. T.; Vasylyev, S.; Peukert, W. *Langmuir* **2010**, *26*, 13564–13571.
- (17) Walther, A.; Muller, A. H. E. *Soft Matter* **2008**, *4*, 663–668.
- (18) Denkov, N. D.; Velev, O. D.; Kralchevsky, P. A.; Ivanov, I. B.; Yoshimura, H.; Nagayama, K. *Langmuir* **1992**, *8*, 3183–3190.
- (19) Dimitrov, A. S.; Nagayama, K. *Langmuir* **1996**, *12*, 1303–1311.
- (20) Kleinert, J.; Kim, S.; Velev, O. D. *Langmuir* **2010**, *26*, 10380–10385.
- (21) Prevo, B. G.; Kuncicky, D. M.; Velev, O. D. *Colloids and Surfaces a-Physicochemical and Engineering Aspects* **2007**, *311*, 2–10.
- (22) Jiang, P.; McFarland, M. J. *J. Am. Chem. Soc.* **2004**, *126*, 13778–13786.
- (23) Lee, Y. L.; Du, Z. C.; Lin, W. X.; Yang, Y. M. *J. Colloid Interface Sci.* **2006**, *296*, 233–241.
- (24) Song, J. H. *Template-Assisted Materials Engineering*; City University of New York: New York, 2009.
- (25) Ossenkamp, G. C.; Kemmitt, T.; Johnston, J. H. *Chem. Mater.* **2001**, *13*, 3975–3980.
- (26) Ishikawa, T.; Matsuda, M.; Yasukawa, A.; Kandori, K.; Inagaki, S.; Fukushima, T.; Kondo, S. *J. Chem. Soc., Faraday Trans.* **1996**, *92*, 1985–1989.
- (27) Kimura, T.; Kuroda, K.; Sugahara, Y. *J. Porous Mater.* **1998**, *5*, 127–132.
- (28) Horozov, T. S.; Aveyard, R.; Clint, J. H.; Binks, B. P. *Langmuir* **2003**, *19*, 2822–2829.
- (29) Kralchevsky, P. A.; Nagayama, K. *Langmuir* **1994**, *10*, 23–36.
- (30) Lvov, Y.; Ariga, K.; Onda, M.; Ichinose, I.; Kunitake, T. *Langmuir* **1997**, *13*, 6195–6203.
- (31) Wang, W.; Gu, B. H. *J. Phys. Chem. B* **2005**, *109*, 22175–22180.
- (32) Wang, W.; Gu, B. H.; Liang, L. Y.; Hamilton, W. J. *J. Phys. Chem. B* **2003**, *107*, 3400–3404.
- (33) Smoukov, S. K.; Gangwal, S.; Marquez, M.; Velev, O. D. *Soft Matter* **2009**, *5*, 1285–1292.
- (34) Duan, H. W.; Wang, D. Y.; Sobal, N. S.; Giersig, M.; Kurth, D. G.; Mohwald, H. *Nano Lett.* **2005**, *5*, 949–952.
- (35) Dimitrov, A. S.; Miwa, T.; Nagayama, K. *Langmuir* **1999**, *15*, 5257–5264.
- (36) Lopez, C. *Adv. Mater.* **2003**, *15*, 1679–1704.